Creating a Small Anchor to Eliminate Large Knots in Mesh and Tape Suture

Jason L. Green
Duke University School of Medicine,
487 Medical Science Research Building 1,
203 Research Drive,
Durham, NC 27710
e-mail: jason.l.green@duke.edu

Richard Glisson
Department of Mechanical Engineering and
Material Science,
Duke University,
P.O. Box 90300,
Durham, NC 27708
e-mail: r.r.glisson@duke.edu

Jane Hung
Optum,
4242 Six Forks Road,
Suite 1100,
Raleigh, NC 27609
e-mail: jane.hung@optum.com

Mohamed Ibrahim
Division of Plastic, Maxillofacial, and Oral Surgery,
Duke University Medical Center,
DUMC 3181,
Durham, NC 27710
e-mail: Mohamed.ibrahim@duke.edu

Alfredo Farjat
Department of Biostatistics and Bioinformatics,
Duke University,
11028F Hock Plaza,
Box 2721,
Durham, NC 27710
e-mail: alfredo.farjat@duke.edu

Beiyu Liu
Department of Biostatistics and Bioinformatics,
Duke University,
11028B Hock Plaza,
Box 2721,
Durham, NC 27710
e-mail: beiyu.liu@duke.edu

Ken Gall
Department of Mechanical Engineering and
Material Science,
Duke University,
Durham, NC 27708;
Edmund T. Pratt Jr. School of Engineering,
Duke University,
Box 90300 Hudson Hall,
Durham, NC 27708
e-mail: kag70@duke.edu

Howard Levinson[1]
Division of Plastic, Maxillofacial, and Oral Surgery,
Duke University Medical Center,
Durham, NC 27710;
Division of Surgical Sciences,
Department of Surgery and Pathology,
DUMC 3181,
Durham, NC 27710
e-mail: howard.levinson@duke.edu

Wide mesh or tape sutures are used to close high-tension wounds such as in hernia or tendon repair. However, wide sutures produce large knots that are susceptible to increased palpability, infection, and foreign body response. To prevent such adverse events, we developed a small suture anchor to replace wide suture knots. The suture anchor was iteratively developed using three-dimensional (3D) design software and produced via 3D printing. Anchor prototypes underwent monotonic, cyclic fatigue, and stress-life testing in a benchtop soft tissue suture model. Results were compared to a standard of care knot and alternative suture fixation devices. The final anchor design was selected based on minimal size and mechanical performance. The size of the final anchor (200 mm^3) was 33% smaller than a tape suture knot and 68% smaller than a mesh suture knot. Monotonic testing of mesh and tape sutures revealed a significantly greater anchor failure load compared to knot and alternative fixations ($p < 0.05$). Additionally, all anchors successfully completed cyclic fatigue testing without failure while other fixations, including knot, failed to complete cyclic fatigue testing multiple times. Stress-life testing demonstrated durable anchor fixation under varying tensile stresses. Failure mode analysis revealed anchor fracture and tissue failure as modes of anchor failure, each of which occurred at supraphysiologic forces. We created a small suture anchor that significantly outperforms knot and alternative suture fixations in benchtop testing and addresses concerns of increased palpability, infection, and foreign body response from large suture knots.
[DOI: 10.1115/1.4040186]

1 Introduction

Wide sutures are used in high-tension tissue closures such as in hernia or tendon repair because they have greater tensile strength [1] and increased resistance to sutures pulling through tissue [2] as compared to standard suture. There are two common types of wide suture: mesh suture and tape suture. Mesh suture was initially investigated by Dumanian et al. to overcome suture pull-through and ensuing recurrence in hernia repair [2,3]. When applied in a swine laparotomy model, mesh suture closure had increased work to failure and increased early wound strength [3]. In human abdominal wall closure, mesh suture provided reliable tissue closure under tension and was associated with low rates of dehiscence, delayed wound healing, and hernia recurrence [4]. Tape suture is a flat, less porous, braided wide suture. An example of tape suture is QuikCord™ tape suture (MedShape, Inc., Atlanta, GA), which is indicated for soft tissue approximation, mainly in orthopedic procedures. Its applications include Achilles tendon reattachment, ligament repair, and hallux valgus reconstruction [5].

Despite the many advantages of wide sutures, a major concern is the large, high-profile knots they create. Large knots are susceptible to increased palpability and foreign body response [6]. Additionally, larger knots have increased area for bacterial adherence and may increase the risk of infection [7,8]. Thus, there is a need for an alternative suture fixation to replace knots in wide sutures. A knotless suture anchor is a device that secures a suture, in lieu

[1]Corresponding author.

Manuscript received September 6, 2017; final manuscript received April 29, 2018; published online July 13, 2018. Assoc. Editor: Chris Rylander.

of a knot, so the suture will not move through tissue. They can also be easier to apply than knots in hard to reach places and may be more effective in areas of high tension where knots may unravel. Examples of suture anchor devices currently on the market include the BIORAPTOR™ Knotless Suture Anchor (Smith & Nephew, Inc., Andover, MA) and the Bio-SutureTak™ Suture Anchor (Arthrex, Inc., Naples, FL). These are classified as orthopedic suture anchors as they fixate soft tissue to bone. Interestingly, there are no suture anchors to fixate soft tissue to soft tissue. To address this deficiency, we developed an innovative small suture anchor for soft tissue fixation. The main design goals of the suture anchor were for it to be low-profile and for it to achieve superior mechanical performance in comparison with a knot and alternative suture fixations.

2 Methodology

2.1 Design and Production. Small suture anchor prototypes were created using FUSION360 (Autodesk, Inc., San Rafael, CA) three-dimensional (3D) design software. Anchor designs were limited in terms of height, width, and application method. An anchor height of $\leq$3 mm was chosen based on the approximate height of a 1–0 suture knot with four throws. Anchor width was limited to $\leq$15 mm to minimize contact with adjacent tissue in vivo. The base design of the anchor comprised two interlocking components to enable application through wide sutures. In accordance with these design requirements, anchor prototypes were iteratively designed with variations in shape, dimensions, locking mechanism, and suture fixation. A Carbon 3D® printer was used to produce multiple anchors simultaneously, enabling mass prototyping. Anchors were printed using UV-curable liquid polymer resins consisting of polyurethane for initial prototyping followed by urethane methacrylate for final design testing. Polyurethane was used for initial prototyping as it is cheaper in comparison with other printer-compatible resins and required minimal processing, allowing for efficient prototype production. Urethane methylacrylate resin was made available later in the study and was selected for final design testing because of similar production time to polyurethane and stronger mechanical properties. After printing, anchors underwent resin-specific curing, washing, and drying protocols to optimize mechanical properties.

2.2 Comparative Performance Testing. Following production, the ability of the prototypes to fixate wide sutures in surrogate soft tissue, specifically to prevent sutures sliding through the suture tract, was compared to a knot and alternative soft tissue suture fixations. Each fixation was applied to a mesh suture and a QuikCord tape suture to undergo performance testing in a benchtop soft tissue suture model. Mesh sutures consisted of a flat, porous polypropylene mesh, approximately 10 mm in width. A width of 10 mm was selected for mesh sutures as this is the median of the widths used in previously published studies involving mesh sutures [2,4]. The QuikCord tape sutures were a flat, braided polyethylene suture, approximately 3.5 mm in width. Force was applied to this model, and the performance was measured using an Instron® machine (model 1321, Illinois Tool Works, Inc., Norwood, MA). Silicone was selected as a soft tissue surrogate tissue during testing to function as a controlled substrate between conditions. We chose silicone as a soft tissue surrogate because it is a homogenous substrate that is consistent between samples, is readily available, easy to work with, and has been used as a soft tissue surrogate for mechanical testing in other studies [9,10]. Specifically, silicone has been used to simulate stress distribution in muscle tissue under concentrated loading [9] and to analyze the compressive and tensile responses of pig skin in comparison with silicone rubbers [10]. The silicone was integrated with a mesh support to increase mechanical integrity. Silicone surrogate tissues were dimensioned at 8 cm × 2 cm × 1 cm. A 7-cm-long mesh or tape suture was introduced through the midpoint of the tissue using a Keith needle, which is used clinically. Each fixation was attached at 1 cm distal to an opposing end of suture with the opposite end clamped in a mechanical vise grip connected to the testing machine at 2 cm from the tissue surface. The surrogate tissue was oriented parallel to the machine's stationary horizontal table. This apparatus was anchored laterally, and upward tension was applied perpendicular to the tissue surface. An example of the experimental model is shown in Fig. 1(*a*).

This model was used to perform monotonic and cyclic fatigue testing. Monotonic testing was designed to determine the maximum fixation strength while cyclic fatigue testing was a measurement of fixation durability. The anchor prototype was optimized and compared to a knot, staple,[2] corkscrew,[3] tack,[4] and strap[5] fixation. The anchor was applied to suture using slip-joint pliers under subjective force until the anchor components were fully approximated. The knot fixation was created along the length of the mesh sutures and tape sutures using an instrument tie in which the initial throw was a square, surgeon's knot followed by three alternating square knots, which is a standard surgical approach. The alternative suture fixations were applied in accordance with manufacturer recommendations. Examples of each fixation application are shown in Fig. 2.

2.3 Monotonic Testing. Following production, anchor prototypes underwent monotonic tensile testing in mesh and tape sutures. Performance of the anchor was compared to knot, staple, corkscrew, tack, and strap fixation. Testing was performed in a benchtop soft tissue suture model using an Instron machine. Six samples were tested for each suture fixation. As there are no ASTM standards for soft tissue fixation testing, ASTM D5034 was selected as a basis for our testing. It is applicable to fabrics produced by knitting and weaving and therefore should be translatable to the sutures used in this study. Additionally, the orientation of the fabric and direction of the tensile force is consistent with our experimental model. In our testing, the suture is the textile fabric which is subjected to monotonic and cyclic tensile forces. Tension was applied upwardly and perpendicular to the tissue surface at a distraction rate of 300 mm/min until failure. Failure load and failure mode were recorded.

2.4 Cyclic Fatigue Testing. The experimental model and conditions were designed as described for monotonic testing, including application of the anchor to mesh and tape suture. Cyclic fatigue testing of the anchor and other fixations was performed using sinusoidal loading at a range of 10 to 20 N (maximum physiologic force on the abdomen is 16 N/cm [11]) at 1 Hz for 200 cycles, followed by a postcyclic pull to failure at a rate of 300 mm/min. Six samples were tested for each suture fixation. Completed cycles for each fixation, postcyclic failure load for anchor, and failure mode were recorded.

2.5 Failure Mode. For monotonic and cyclic fatigue testing, the anchor failure modes for all 12 anchor fixation samples were recorded in addition to their respective failure loads. Failure was defined as unimpeded suture movement through the suture tract. The types of failure modes documented were anchor failure (fracture or disassembly), tissue failure, and suture failure. Disassembly was when the anchor components detached. Tissue failure was a defect development in the silicone substrate. Suture failure was a defect development (ex: tearing or fraying) in the suture. These failure modes were used to guide anchor design.

2.6 Size Comparison. The size of the anchor was compared to a QuikCord tape suture and mesh suture knot, each four throws.

[2]Endo Universal™ 65 Hernia Stapler (Medtronic, Inc., New Haven, CT).
[3]ProTack™ Fixation Device (Medtronic, Inc., New Haven, CT).
[4]OptiFix™ Absorbable Fixation System (Davol, Inc., Warwick, RI).
[5]ETHICON SECURESTRAP™ Absorbable Fixation Device (Ethicon, LLC., Guaynabo, PR).

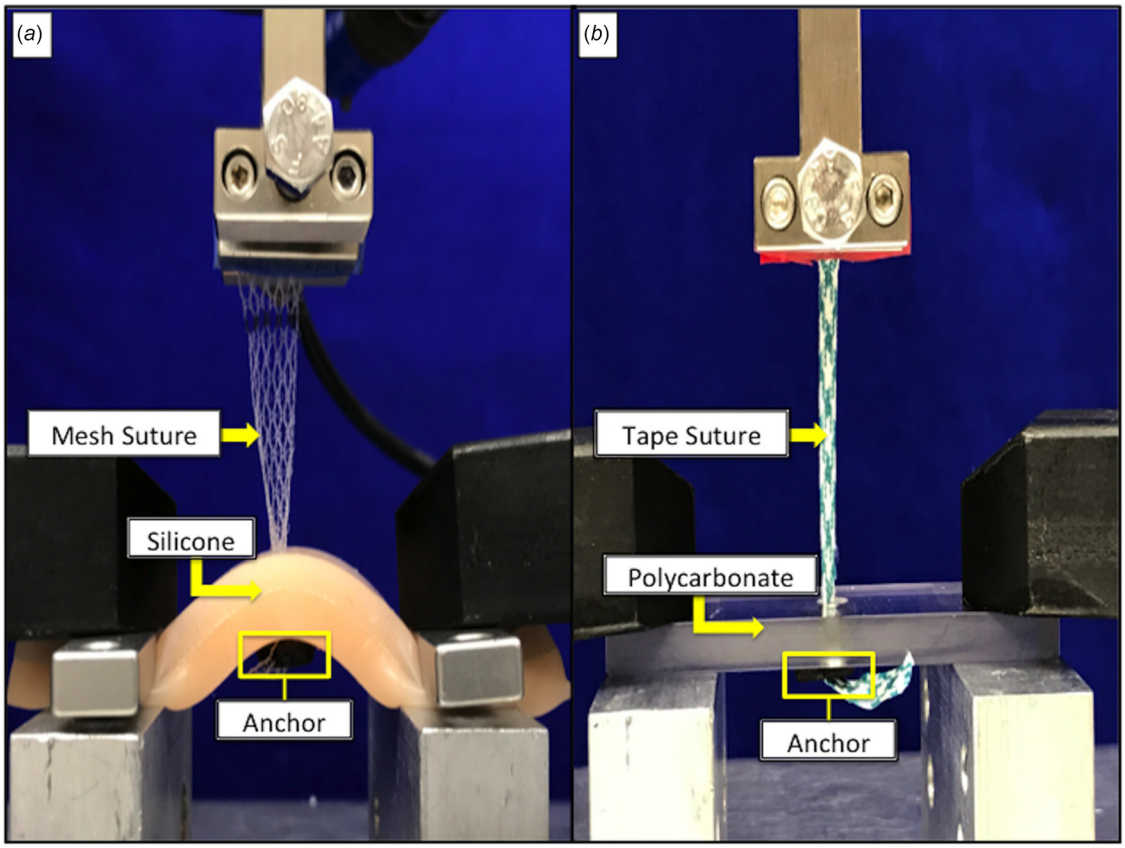

Fig. 1 Setup for monotonic, cyclic fatigue, and stress-life testing. Benchtop model for (*a*) monotonic and cyclic fatigue testing utilizing silicone and (*b*) stress-life testing using polycarbonate.

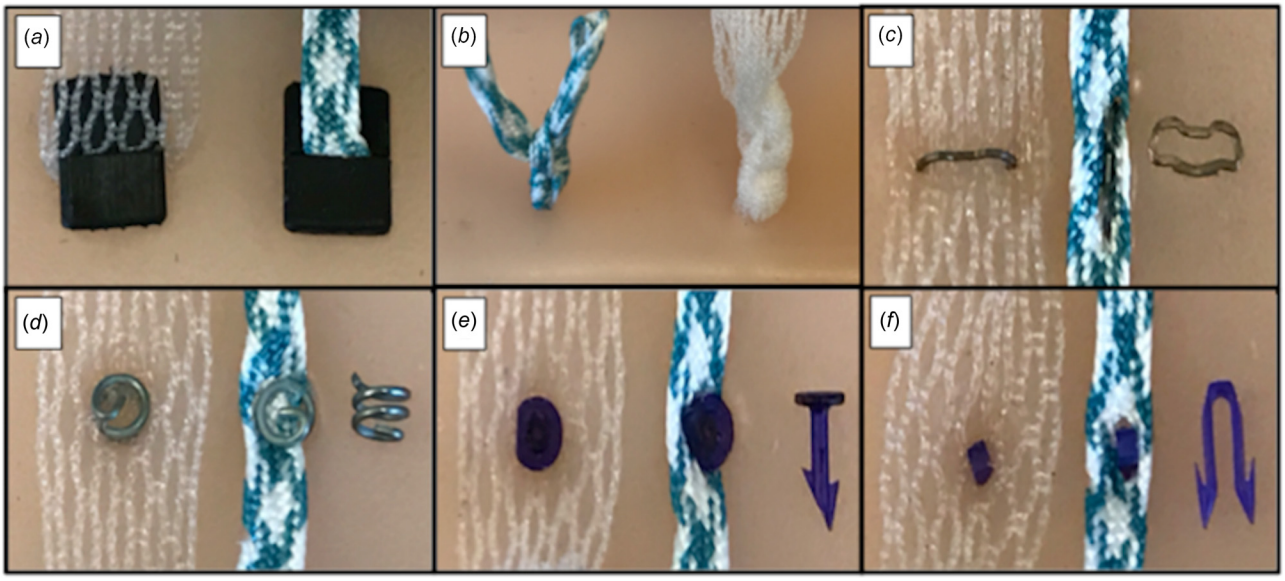

Fig. 2 Mesh and tape suture fixation devices. Representations of how the anchor and each control fixation device were applied to mesh and tape suture for performance testing. (*a*) Anchor, (*b*) knot, (*c*) staple, (*d*) corkscrew, (*e*) tack, and (*f*) strap.

The length, width, and height of each fixation was measured and used to calculate their respective volumes.

2.7 Stress-Life Testing. Stress-life testing was performed on the final anchor in a benchtop polycarbonate suture model. This testing was used to determine the durability of the anchor when exposed to varying degrees of cyclic tension. This specifically measured the fatigue strength of the anchor, which is the highest stress at which the anchor can maintain suture fixation for a given number of cycles. Similar to the monotonic and cyclic protocols, testing consisted of attaching the anchor to a suture (tape suture was used). Next, the suture was passed through a through a 4-mm-diameter hole in a rigid 6-mm-thick polycarbonate substrate and the opposing suture end was connected to the Instron machine. A rigid substrate was selected for its noncompliance, which functioned to isolate anchor performance rather than test the integrity

of the substrate. An example of the experimental model is shown in Fig. 1(*b*).

Sinusoidal stresses were applied to the anchor. Stress levels were determined based on prior monotonic testing of the anchor in the benchtop polycarbonate suture model. Testing parameters were as previously described in the benchtop soft tissue suture model, with a polycarbonate substrate used instead of silicone. The sinusoidal stresses applied were based on a range of percentages (20–95%) of the monotonic failure load from prior testing (117±9 N) at a frequency of 10 Hz. Six anchor fixation samples underwent testing at each sinusoidal stress level. Failure cycle was recorded and used to create a plot of stress amplitude versus number of cycles completed. We selected 100,000 cycles as our upper limit for testing.

2.8 Statistical Analysis. Continuous variables such as monotonic failure load, the number of cycles completed, and the post-cyclic failure load were summarized by reporting their mean, standard deviation, minimum, maximum, and interquartile range. Given that the sample size is relatively small, the nonparametric Wilcoxon rank sum test was used to compare the measures and center of tendency between the continuous variables. Bonferroni correction was employed to account for the family-wise error rate when performing multiple comparisons. In all cases, the threshold for assessing statistical significance was set at level $\alpha = 0.05$. Analyses were conducted in SAS statistical software version 9.4 (SAS Institute Inc., Cary, NC).

3 Results

3.1 Anchor Design. The final anchor was selected based on minimal size and superior mechanical performance. The final anchor design (Fig. 3(*c*)) consisted of two interlocking male/female components. The male component included two lateral projections and a middle projection along the midline surface. The middle projection provided primary suture fixation via penetration through suture and joining into the female component. The middle projection was tapered distally to enable penetration through wide suture. The two lateral projections featured a locking element to enable locking when attached to the female component. In addition to locking, the lateral projections also penetrated the wider mesh suture, assisting in mesh suture fixation. The female component consisted of corresponding holes to allow entry and internal recesses to enable locking of the male projections. An example of how the anchor is applied to mesh and tape sutures is shown in Fig. 4.

3.2 Size Comparison. The sizes of the suture fixations, as measured by volume, were as follows: anchor-200 mm^3, tape suture knot-300 mm^3, and mesh suture knot-630 mm^3. The anchor size was 33% smaller than a tape suture knot and 68% smaller than a mesh suture knot. The dimensions of the anchor are shown in Figs. 5(*a*) and 5(*b*) while a side-by-side comparison of the anchor versus suture knots is shown in Fig. 5(*c*).

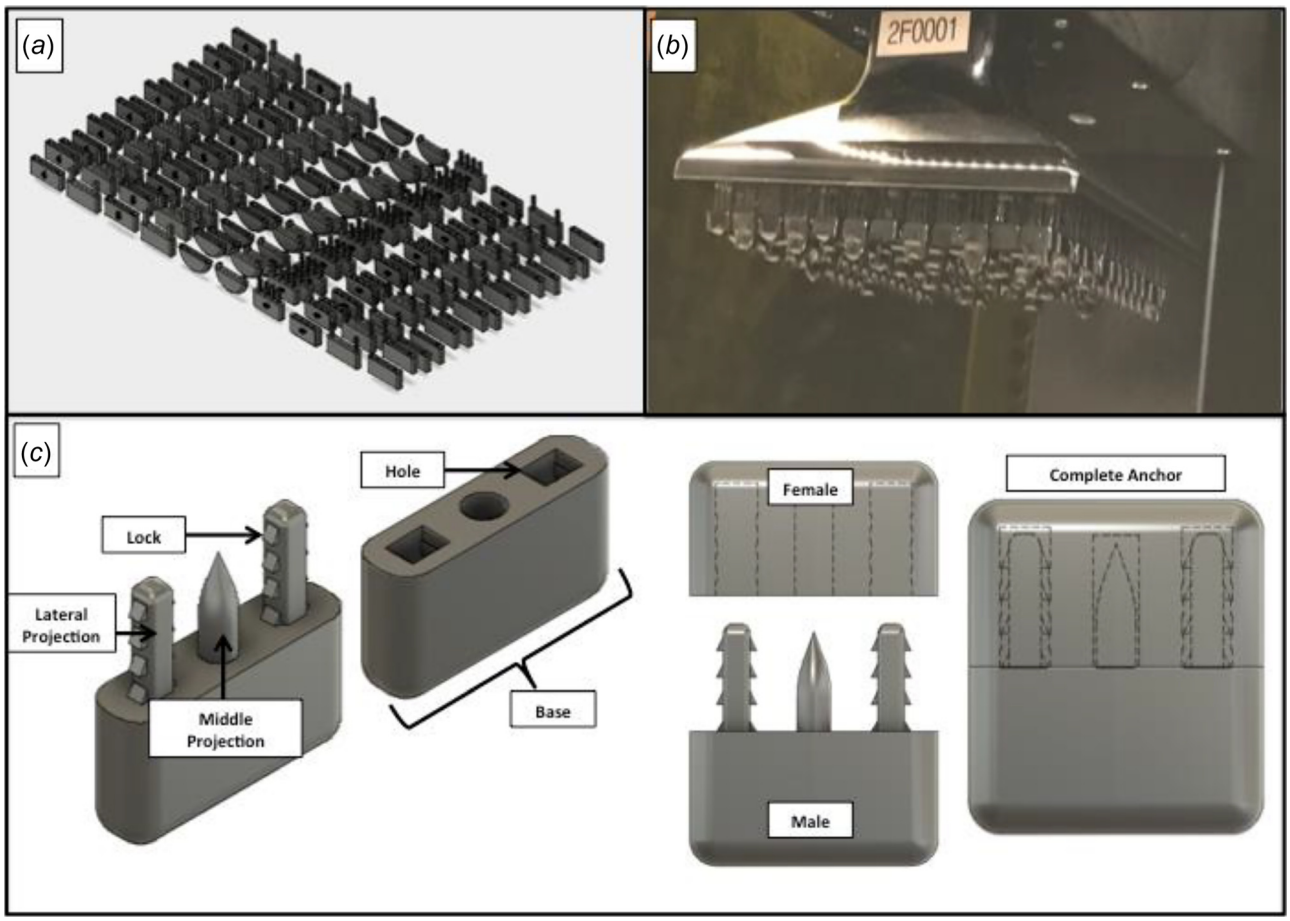

Fig. 3 Prototype iteration and final anchor design. (*a*) Example of 3D design iterations of various anchor prototypes made using FUSION360 software. (*b*) Anchor prototypes were produced by 3D printing using a Carbon 3D® printer. (*c*) The final anchor consists of two interlocking male/female components. The male component has two lateral locking projections and a single midline projection that provides primary suture fixation. The middle projection penetrates through large suture and joins into the female component. This enables suture fixation at the anchor–tissue interface. In addition to locking, the lateral projections provide secondary suture fixation in mesh sutures.

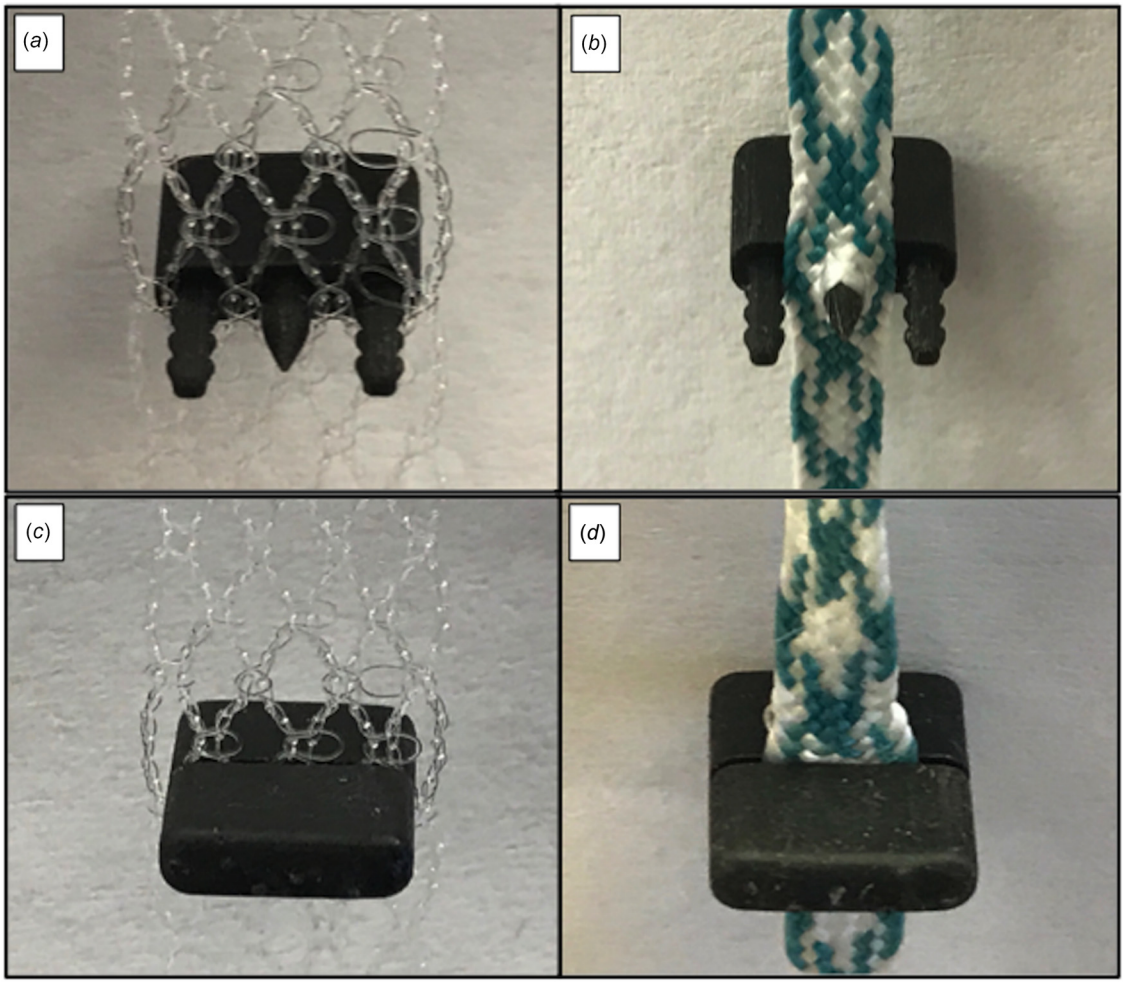

Fig. 4 Anchor application to mesh and tape sutures. (*a*) and (*b*) demonstrate the application of the male component into mesh and tape sutures, respectively. (*c*) and (*d*) demonstrate the joining of the male and female components around the suture, creating the complete anchor fixation.

3.3 Monotonic Testing. For monotonic testing in the benchtop soft tissue suture model, the final anchor design had a significantly greater anchor failure load than the other fixations in both mesh and tape sutures. In mesh sutures, the anchor failure load (49±4 N) exceeded knot (32±14 N), staple (14±3 N), corkscrew (12±8 N), tack (18±4 N), and strap (19±5 N) fixation ($p < 0.05$, $n = 6$) (Fig. 6(*a*)). In tape sutures, the anchor failure load (49±7 N) was greater than knot (22±5 N), staple (13±6 N), corkscrew (11±11 N), tack (23±4 N), and strap (13±3 N) fixation ($p < 0.05$, $n = 6$) (Fig. 6(*b*)).

3.4 Cyclic Fatigue Testing. In mesh sutures, the average number of cycles completed was as follows: anchor-200±0 cycles, knot-133±103 cycles, strap-134±103 cycles, corkscrew-36±80 cycles, tack-1±2 cycles, and staple-0±0 cycles. The cycles completed for the anchor in mesh sutures were significantly greater than in staple and tack fixations ($p < 0.05$, $n = 6$) (Fig. 7(*a*)). In tape sutures, the average number of cycles completed was as follows: anchor-200±0 cycles, knot-103±106 cycles, strap-1±1 cycle, corkscrew-69±102 cycles, tack-57±89 cycles, and staple-0±0 cycles. The cycles completed for the anchor in tape sutures were significantly greater than in staple and strap fixations ($p < 0.05$, $n = 6$) (Fig. 7(*b*)). In both suture types, the anchor was the only fixation that consistently completed cyclic testing.

The postcyclic failure loads of the anchor were compared to the previously measured monotonic failure loads in both suture types. For mesh sutures, the difference between the monotonic (49 ± 4 N) and postcyclic (43 ± 4 N) failure loads was statistically significant ($p < 0.05$, $n = 6$). For tape sutures, the monotonic (496 ± 7N) and postcyclic (436 ± 5N) failure loads were not significantly different ($p = 0.13$, $n = 6$).

3.5 Failure Mode. Examples of each failure mode are shown in Fig. 8(*a*). The primary modes of failure in mesh sutures were anchor fracture (50%) and tissue failure (50%) ($n = 12$) (Fig. 8(*b*)). In tape sutures, the only failure mode was anchor fracture (100%) ($n = 12$) (Fig. 8(*c*)). In mesh sutures, anchor fracture occurred at 49±4 N and tissue failure at 44±5 N. In tape sutures, anchor fracture took place at 46±6 N.

3.6 Stress-Life Testing. Stress-life testing demonstrated a consistent negative correlation between stress and completed cycles. The maximum stress amplitude was 50.3 N (corresponding to a sinusoidal load of 60.3 N to 110.6 N)) at which 12±15 cycles were completed. The minimum stress amplitude was 12.5 N (load 22.4 N to 34.9 N) at which the anchor completed 100,000±0 cycles ($n = 6$) (Fig. 9).

4 Discussion

The size of the final anchor (200 mm^3) was 33% smaller than a tape suture knot and 68% smaller than a mesh suture knot. The anchor significantly outperformed wide suture knots and alternative fixations in monotonic testing. In cyclic fatigue testing, it

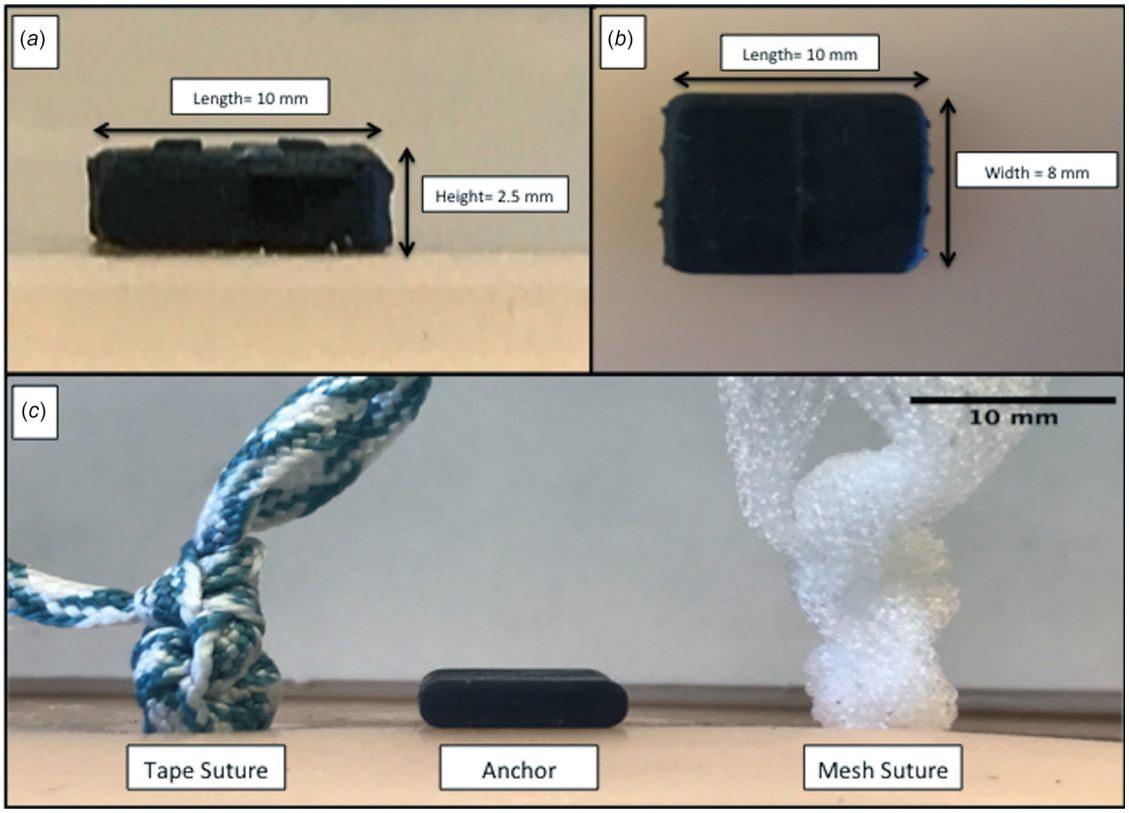

Fig. 5 Size comparison. (*a*) Anchor height is 2.5 mm and length is 10 mm. (*b*) Anchor width is 8 mm. (*c*) Volume comparisons of QuikCord tape suture, innovative anchor, and mesh suture. The anchor size is 33% smaller than a tape suture knot and 68% smaller than a mesh suture knot.

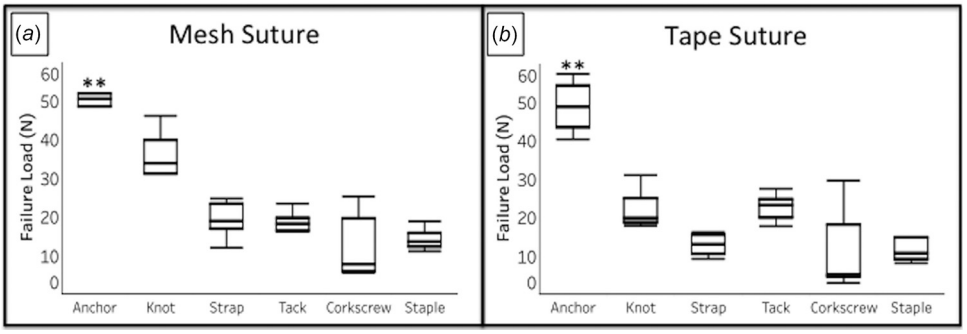

Fig. 6 Monotonic performance of fixation devices in mesh and tape suture. (*a*) In mesh sutures, the anchor had a significantly greater failure load (49±4 N) compared to knot (32±14 N), staple (14±3 N), corkscrew (12±8 N), tack (18±4 N), and strap (19±5 N) fixations ($p < 0.05$, $n = 6$). (*b*) In tape sutures, the anchor failure load (49±7 N) was significantly greater than knot (22±5 N), staple (13±6 N), corkscrew (11±11 N), tack (23±4 N), and strap (13±3 N) ($p < 0.05$, $n = 6$).

performed significantly greater than multiple fixations. Although it did not significantly outperform knot fixations, the anchor was the only fixation to complete all cyclic testing trails. As a result, the anchor had no deviation in its cyclic performance while other fixations had variable numbers of cycles completed, indicating a unique reliability with anchor fixation. This can be clinically significant as the anchor's consistent durability in benchtop testing may translate to durable suture fixation inside the body. Monotonic and postcyclic anchor failure loads were significantly different in mesh sutures while being similar in tape sutures. While significantly different in mesh sutures, the actual difference was less than 10 N and remained greater than the failure loads of other fixations. Stress-life testing further demonstrated durable suture fixation under varying tensile stress. Failure mode analysis revealed anchor fracture and tissue failure as modes of failure. Ultimately, we were able to design, produce, and mechanically test a novel suture anchor that is smaller in size than wide suture knots while mechanically outperforming knots and alternative forms of soft tissue suture fixation.

The smaller size of our anchor was accomplished through 3D design and 3D printing. The FUSION360 software enabled 3D design of a suture anchor to specified shapes and dimensions, with each design being smaller than a wide suture knot. The Carbon 3D® printer provided rapid and accurate production of anchor prototypes according to the specifications of our designs that were strong enough for mechanical testing. These tools together created

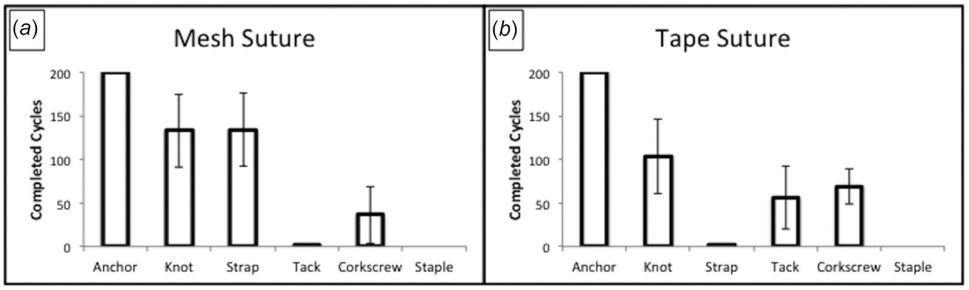

Fig. 7 Cyclic fatigue testing of fixation devices in mesh and tape sutures. (*a*) In mesh sutures, the anchor (200 cycles) completed more cycles in comparison with knot (133), strap (134), tack (1), corkscrew (36), and staple (0) fixations ($n = 6$). (*b*) In tape sutures, the anchor (200 cycles) also completed more cycles in comparison with knot (103), strap (1), tack (57), corkscrew (69), and staple (0) fixations ($n = 6$). The anchor was the only fixation to complete cyclic testing in both suture types.

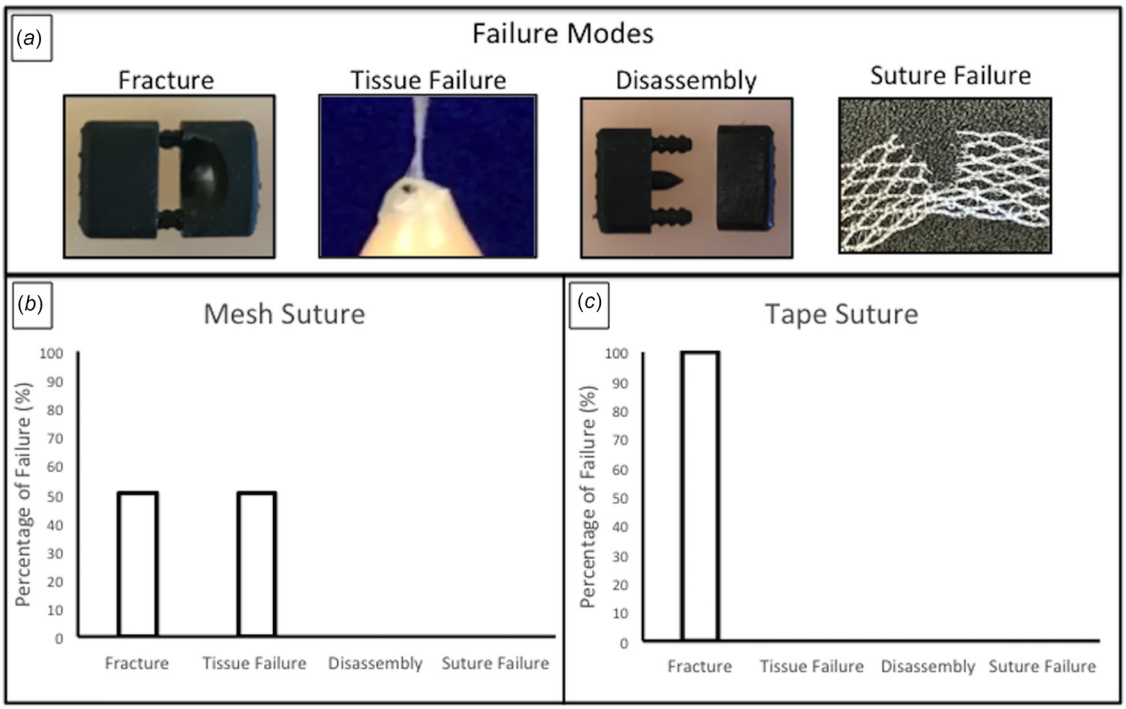

Fig. 8 Failure mode analysis. (*a*) The primary modes of failure in mesh sutures were anchor fracture (50%) and tissue failure (50%) ($n = 12$). (*b*) In tape sutures, the only failure mode was anchor fracture (100%) as tissue failure, disassembly, and suture failure did not occur ($n = 12$). Each of these failure modes occurred at supraphysiologic (> 16 N/cm) forces.

an iterative design and prototyping process that consistently produced a suture anchor smaller than a wide suture knot.

Superior mechanical performance was achieved through the ability of the anchor fixation to resist multiple modes of failure throughout mechanical testing. Suture fixation can be divided into three components: fixation, suture, and tissue. Each of these components can become a source of failure of the construct. Therefore, the three failure modes we distinguished in testing were fixation failure (anchor failure), suture failure, and tissue failure.

The two ways in which the anchor could fail were fracture or disassembly. Anchor fracture consistently occurred at the projections at an average force of 49 ± 4 N in mesh sutures and 46 ± 6 N in tape sutures. The resistance to anchor fracture can be explained using flexural mechanics. Flexural strength is the ability to resist breaking under bending force. This is a critical parameter in the anchor as the load bearing projections experience bending stress when tension is applied to sutures. Flexural strength was a consideration in our material choice. While material selection was limited to printer-compatible liquid polymer resins, there were several prototyping and final production resins from which to choose. We selected urethane methacrylate because of low-cost, quick processing, and its flexural properties. It possesses a flexural stress of 79 ± 5 MPa and a flexural modulus of 2010 ± 119 MPa [12], allowing the projections to sustain high bending stress without fracture during testing. Additionally, the final anchor design features multiple projections across the midline surface of the male component. Multiple projections distribute the flexural force across each other and further prevent anchor fracture. Disassembly did not occur throughout mechanical testing. The lateral projections of the male component were equipped with ridges designed to snap into internal recesses within the female component. This created three bilateral locks along the length of each projection to resist disassembly.

Suture failure did not occur in our studies. This is due to the tensile properties of the sutures and the anchor–suture relationship. The mesh suture is a porous suture made of interconnected

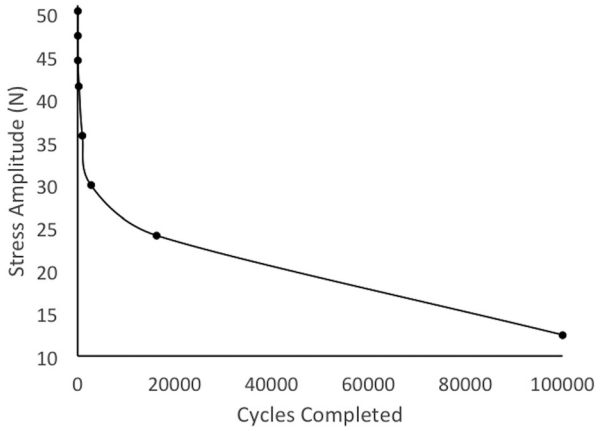

Fig. 9 Stress-life testing of anchor in tape sutures. The maximum stress amplitude was 50.3 N (corresponding to a sinusoidal load of 60.3–110.6 N) at which 12 cycles were completed. The minimum stress amplitude was 12.5 N (load 22.4 N to 34.9 N) at which the anchor life exceeded 100,000 cycles ($n = 6$).

polypropylene fibers while the QuikCord tape suture is less porous braided construct made of polyethylene. Each demonstrated sufficient tensile strength to resist failure under the stresses applied during testing. In regard to the anchor–suture relationship, the anchor's middle projection was able to penetrate both suture types without affecting tensile strength. This is secondary to tapering the distal projection for easy integration and a smooth surface to minimize suture damage.

Tissue failure only occurred in mesh suture at an average failure load of 44 ± 5 N. To establish clinical relevance, the maximum physiologic force exerted on the abdominal wall after surgery is 16 N/cm [11]. This makes tissue failure supraphysiologic and begins to establish a clinical application of the anchor to abdominal closure. This result can be explained by force distribution at the anchor–tissue interface. The anchor is in contact with the tissue surface but does not penetrate tissue. Rather, it distributes a compressive force across the tissue surface when tension is applied. This anchor–tissue interface is 80 mm^2, which appears to sufficiently distribute force and reduce pressure per unit area of tissue. Ultimately, this decreases propensity for tissue failure.

However, the ability to translate these results clinically is limited by the use of silicone gel as a soft tissue surrogate instead of human tissue. Although silicone functioned as a controlled substrate for testing, it lacks the heterogeneity of human tissue, has increased dryness, and is more compliant. The dryness of silicone may result in more friction at the anchor–tissue interface then would occur in living tissue. The increased compliance in silicone may also result in more tissue deformation and a higher propensity for tissue failure in comparison with human tissue. These differences indicate a need for future validation testing in a cadaver model to more accurately simulate living tissue. However, at this point a synthetic tissue is superior for determining relative device strength due to increased substrate repeatability.

The mechanical performances of the suture knots were inferior to the anchor in all comparative testing. Similar to the anchor, the knot forms an obstruction at the tissue interface that prevents suture movement when tension is applied. In this model, the integrity of the obstruction and the area of the obstruction–tissue interface determine performance. Integrity of the knot is dependent on the type of knot [13], number of throws [14], and skill of the performer. The area of the knot–tissue interface is dependent on the length and width of the knot. A larger area distributes force and increases resistance to tissue failure. However, this area is limited by the suture size, as additional knot throws mainly affect knot height. Therefore, more throws would likely only increase the risk of the complications related to knot size.

The alternative knotless fixations we tested were selected based on their clinical application to soft tissue fixation. While not specifically used for suture, each is indicated for the fixation of prosthetic material or mesh to soft tissue, including abdominal wall repair. This is similar to the indications for our suture anchor, which is to fixate wide sutures in soft tissue applications. Therefore, these fixations were chosen as the most representative clinical comparisons to our device. All knotless fixations performed significantly worse than the suture anchor in monotonic testing while multiple were significantly outperformed in cyclic testing. The primary failure mode across alternative fixations was tissue failure in which there was silicone damage and the fixation remained attached to sutures. This can be explained by the fixation–tissue relationship. Each fixation pierced the tissue and stabilized using a hook, screw, or barb mechanism. By anchoring within the tissue, these iterations created a minimal area for the fixation–tissue interface. This concentrated force resulting in early tissue failure when tension was applied.

Our study design consisted of a controlled, experimental setup that isolated suture fixation in a model translatable to high-tension soft tissue closure. The tissue surrogate, suture type, and tensile force remained consistent across fixation types. Additionally, tensile force was applied perpendicular to the tissue surface. This directionality ensured that the suture applied negligible force to the tissue, minimizing suture contribution to tissue failure. Our choices of comparison were representative of the standard of care and potential competitor devices. The mechanical tests enabled comparison of maximum fixation strength, durability under physiological forces, and the anchor's fatigue strength under varying tension.

Limitations to the study included the use of silicone as a soft tissue surrogate which lacks the mechanical properties and heterogeneity of human tissue. Additionally, silicone also differs from human tissue in terms of dryness and compliance. The dryness of silicone may result in more friction at the anchor–tissue interface then occurring in living tissue. The increased compliance in silicone may also result in more tissue deformation and a higher propensity for tissue failure in comparison with human tissue. These differences indicate a need for future validation testing in a cadaver model to more accurately simulate living tissue. Another limitation is the direction of tension on the suture. While we applied tension perpendicular to the tissue surface, directionality may be more variable in vivo depending on positioning, pressure, and muscle usage.

We also chose not to compare performance between different materials used for the anchor. This is due to the limited materials available for 3D printing and the high resolution required to print individual anchor components. The Carbon 3D® printer limits material options to a selection of UV-curable liquid resins, few of which were applicable to the anchor's function. Of the materials that were suitable, we chose not to perform comparisons as the urethane-methylacrylate and polyurethane resins were the only materials able to accurately print the holes of the anchor's female component. Another limitation of the study was the variation in anchor application. The anchor was applied manually so the robustness of its application varied between individuals. Therefore, a future objective is to develop an automated anchor applicator for open and laparoscopic application to minimize anchor application variability.

Despite the limitations secondary to study design, anchor material, and application, the work described here produced a novel form of suture fixation. The suture anchor is a low-profile fixation applicable to wide sutures in soft tissue closure and approximation. As it is much smaller than a suture knot, it could reduce the risk of clinical complications including palpability, foreign body response, and infection. Its superior mechanical performance to alternative fixations should also translate to a more reliable suture fixation in vivo.

However, the current material being used to produce the anchor is not appropriate for clinical use. The final material should have

the appropriate physical and mechanical properties and be biocompatible. This includes completing toxicity testing such as cytotoxicity, genotoxicity, sensitization, irritation, and hemocompatibility. Ideally, the final anchor will be produced in a previously Food and Drug Administration-approved material, which should increase the likelihood of successfully meeting biocompatibility standards. Possible materials include but are not limited to degradable polylactic acid (PLA) and nondegradable polyether ether ketone (PEEK). PLA is a biodegradable thermoplastic used clinically for mesh fixation to soft tissue [15,16]. A PLA-based anchor would degrade and therefore not require postoperative anchor removal. PEEK is a nonabsorbable thermoplastic polymer used in orthopedic suture anchors [17] and medical implants such as spinal fusion devices [18]. Given that PEEK and PLA differ in both absorbability and mechanical properties, further testing will be required to compare their respective anchor performances.

Clinically, the anchor will be coupled with an applicator to ensure consistent application to suture. This applicator will also feature a removal function for safe anchor detachment if improperly placed. The postoperative management of the anchor will be material dependent. A nondegradable material could require later removal if there were complications but not necessarily as many nondegradable implants are left within the patient indefinitely. A degradable material should not require a secondary operation.

Future work will consist of producing the anchor in Food and Drug Administration-approved biocompatible materials followed by comparative testing in cadaveric tissue. The results of these tests will determine which material will be used to produce anchors for application in an animal model. The animal model will examine the utility of the anchor in high-tension soft tissue closure, specifically hernia and tendon repair. This will prelude evaluation of clinical performance and analysis of the complications related to large knots.

5 Conclusions

The suture anchor device described here is smaller in size than wide suture knots while mechanically outperforming knots and alternative forms of wide suture fixation in a benchtop soft tissue suture model. Future efforts are required to select a final material, design an applicator, and to perform cadaveric and animal model testing. The design and current data provide the foundation for a novel suture anchor to replace wide suture knots in high-tension soft tissue suture fixation, which may include hernia and tendon repair.

Acknowledgment

Thank you to the following individuals for their contributions to this project and manuscript: Dr. Bruce Klitzman of the Duke University Department of Biomedical Engineering, Eric Stach of the Duke University Department of Mechanical Engineering and Materials Science, and Dr. David Ruppert. Dr. Levinson is supported by the NC Biotechnology Center Small Business Research Loan and the Duke University Department of Surgery. These funders were not involved in the design or completion of this study; data collection or interpretation; or preparation or review of this manuscript. Dr. Levinson is the founder of Deep Blue Medical Advances who has licensed this technology from Duke University.

Funding Data

- Duke University (Department of Surgery).
- North Carolina Biotechnology Center (Small Business Research Loan).

References

[1] Gnandt, R. J., Smith, J. L., Nguyen-Ta, K., McDonald, L., and LeClere, L. E., 2016, "High-Tensile Strength Tape Versus High-Tensile Strength Suture: A Biomechanical Study," Arthroscopy, **32**(2), pp. 356–63.

[2] Souza, J. M., Dumanian, Z. P., Gurjala, A. N., and Dumanian, G. A., 2015, "In Vivo Evaluation of a Novel Mesh Suture Design for Abdominal Wall Closure," Plast. Reconstr. Surg., **135**(2), pp. 322e–330e.

[3] Dumanian, G. A.,Tulaimat, A., and Dumanian, Z. P., 2015, "Experimental Study of the Characteristics of a Novel Mesh Suture," Br. J. Surg., **102**(10), pp. 1285–1292.

[4] Lanier, S. T., Dumanian, G. A., Jordan, S. W., Miller, K. R., Ali, N. A., and Stock, S. R., 2016, "Mesh Sutured Repairs of Abdominal Wall Defects," Plast. Reconstr. Surg. Global Open, **4**(9), p. e1060.

[5] Smith, K. E., Dupont, K. M., Safranski, D. L., Blair, J., Buratti, D., Zeetser, V., Callahan, R., Lin, J., and Gall, K., 2017, "Use of 3D Printed Bone Plate in Novel Technique to Surgically Correct Hallux Valgus Deformities," Tech. Orthop., **31**(3), pp. 181–189.

[6] van Rijssel, E. J., Brand, R., Admiraal, C., Smit, I., and Trimbos, J. B., 1989, "Tissue Reaction and Surgical Knots: The Effect of Suture Size, Knot Configuration, and Knot Volume," Obstet. Gynecol., **74**(1), pp. 64–68.

[7] Alexander, J. W., Kaplan, J. Z., and Altemeier, W. A., 1967, "Role of Suture Materials in the Development of Wound Infection," Ann. Surg., **165**(2), pp. 192–199.

[8] Masini, B. D., Stinner, D. J., Waterman, S. M., and Wenke, J. C., 2011, "Bacterial Adherence to Suture Materials," J. Surg. Educ., **68**(2), pp. 101–104.

[9] Sparks, J. L., Vavalle, N. A., Kasting, K. E., Long, B., Tanaka, M. L., Sanger, P. A., Schnell, K., and Conner-Kerr, T. A., 2015, "Use of Silicone Materials to Simulate Tissue Biomechanics as Related to Deep Tissue Injury," Adv. Skin Wound Care, **28**(2), pp. 59–68.

[10] Shergold, O. A., Fleck, N. A., and Radford, D., 2006, "The Uniaxial Stress Versus Strain Response of Pig Skin and Silicone Rubber at Low and High Strain Rates," Int. J. Impact Eng., **32**(9), pp. 1384–1402.

[11] Brown, C. N., and Finch, J. G., 2010, "Which Mesh for Hernia Repair?," Ann. R. Coll. Surg. Engl., **92**(4), pp. 272–278.

[12] Carbon, 2017, "UMA 90: Technical Data Sheet," Carbon, Redwood City, CA, accessed Aug. 7, 2017, http://www.carbon3d.com/materials/uma-urethanemethacrylate

[13] Zhao, C., Hsu, C. C., Moriya, T., Thoreson, A. R., Cha, S. S., Moran, S. L., An, K. N., and Amadio, P. C., 2013, "Beyond the Square Knot: A Novel Knotting Technique Surgical Use," J. Bone Jt. Surg. Am., **95**(11), pp. 1020–1027.

[14] Komatsu, F., Mori, R., and Uchio, Y., 2006, "Optimum Surgical Suture Material and Methods to Obtain High Tensile Strength at Knots: Problems of Conventional Knots and the Reinforcement Effect of Adhesive Agent," J. Orthop. Sci., **11**(1), pp. 70–74.

[15] Guerron, A. D., Lee, H. J., Yoo, J., Seymour, K., Sudan, R., Portenier, D., and Park, C., 2017, "Laparoscopic Single-Site Inguinal Hernia Repair Using a Self-Fixating Mesh," JSLS, **21**(1), p. e2016.

[16] Bard, 2017, "OptiFix™ Open Absorbable Fixation System," Bard, Warwick, RI, accessed Aug. 7, 2017, https://www.crbard.com/davol/en-US/products/OptiFix-Open-Absorbable-Fixation-System

[17] Arthrex, 2017, "Suture Anchors," Arthrex, Naples, FL, accessed Aug. 7, 2017, https://www.arthrex. com/hip/suture-anchors

[18] Liao, J. C., Niu, C. C., Chen, W. J., and Chen, L. H., 2008, "Polyetheretherketone (PEEK) Cage Filled With Cancellous Allograft in Anterior Cervical Discectomy and Fusion," Int. Orthop., **32**(5), pp. 643–648.